

Effect of Anomalous Dynamics on Unbiased Polymer Translocation

Debabrata Panja

Institute for Theoretical Physics, Universiteit van Amsterdam, Valckenierstraat 65, 1018 XE Amsterdam, The Netherlands

Gerard T. Barkema

Institute for Theoretical Physics, Universiteit Utrecht, Minnaertgebouw, Leuvenlaan 4, Postbus 80.195, 3508 TD Utrecht, The Netherlands

Robin C. Ball

Department of Physics, University of Warwick, Coventry CV4 7AL, UK

In this paper, we investigate the microscopic dynamics of a polymer translocating through a narrow pore. We find that the dynamics of the polymer is anomalous: in the sense that it *cannot* be described by a Fokker-Planck (which only takes into account the diffusive and drift motions) or Fokker-Planck type equations, although both have been widely used as the starting point for quantitative (mean-field) theoretical analysis of translocation. The idea that translocation dynamics may be anomalous is not new; nevertheless, this work develops a direct characterization method for it for the first time. We show that from the characteristics of the anomalous dynamics of the polymer, it is possible to obtain the scaling of the mean dwell time, the typical time the polymer spends within the pore, with polymer length N . As we do so, we confirm, in a robust manner, our earlier result that the mean dwell time for unbiased translocation scales as $\sim N^{2.4 \pm 0.05}$, which has remained in contradiction to the existing mean-field theory results.

I. INTRODUCTION

Transport of molecules across cell membranes is an essential mechanism for life processes. These molecules are often long, and the pores in the membranes are too narrow to allow the molecules to pass through as a single unit. In such circumstances, the molecules have to deform from their equilibrium conformations in order to squeeze — i.e., translocate — themselves through the pores. DNA, RNA and proteins are such naturally occurring long molecules (1; 2; 3; 4; 5) in a variety of biological processes. Translocation is also used in gene therapy (7; 8), in delivery of drug molecules to their activation sites (9; 10), and as a cheaper alternative for single-molecule DNA or RNA sequencing [see Ref. (6) and the references cited therein]. Understandably, the process of translocation has been an active topic of current research: not only because it is a cornerstone of many biological processes, but also due to its relevance for practical applications.

Translocation is a complicated process in living organisms — the presence of chaperon molecules, pH, chemical potential gradients, and assisting molecular motors strongly influence its dynamics. Consequently, the translocation process has been empirically studied in great variety in biological literature (11; 12). Study of translocation as a *biophysical* process is however more recent. Herein, the polymer is simplified to a sequentially connected string of N monomers as it passes through a narrow pore on a membrane. The quantities of interest for the translocation process are the typical time-scale for the polymer to leave a confining cell (the “escape of a polymer from a vesicle” time scale) (13), and the typical

time scale the polymer spends in the pore (the “dwell” time-scale) (14) as a function of N and parameters like membrane thickness, membrane adsorption, pore size, electrochemical potential gradient etc. (15; 16).

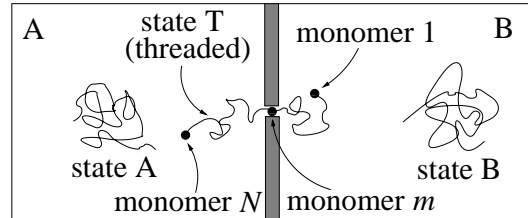


FIG. 1 Our system to study translocation in this paper. It consists of two cells A and B that are connected by a pore of diameter unity in a membrane of thickness unity. Both cells have the same volume V . The polymer repeatedly moves back and forth from one cell to the other through the pore. At any time, exactly one monomer can be within the pore. The Kuhn length of the polymer and the lattice spacing are also set to unity. Polymers can be in three different states (i) state A: all monomers are in cell A; (ii) state T (threaded): some monomers are in cell A and the rest in cell B; (iii) state B: all monomers are in cell B.

These quantities have been measured directly in numerous experiments (17). A number of (mean-field type) theories have been proposed for the scaling of these typical times (13; 14; 15) during the last decade as well. They described translocation as a first-passage or Kramer’s problem over an entropic barrier in terms of the “reaction coordinate” m alone, which could be described by a Fokker-Planck equation. Here m is the number of the monomer threaded into the pore ($m = 1, \dots, N$; see Fig.

1), and the transition rates from m to $m \pm 1$ and vice versa are obtained from the derivatives of the free energy w.r.t. m . In the context of unbiased polymer translocation (i.e., in the absence of external driving fields), the prediction of the mean-field theories (which only considered polymers with simple random walk statistics) was that the mean dwell time scales as N^3 for Rouse dynamics and as $N^{2.5}$ for Zimm dynamics (14). While these theories do indeed provide insight into the process of translocation, their usage of the (equilibrium) free energy to determine the transition rates from m to $m \pm 1$ implicitly assumed that at a fixed reaction coordinate m , the polymers equilibrate much faster than the typical time for the reaction coordinate to change its value by ± 1 .

This (implicit) assumption further implies that the equilibration time of a polymer during translocation is much smaller than its dwell time. The veracity of this statement, in relation to the applicability of the mean-field theories to describe translocation, has recently been questioned (18). Resolution of this issue using computer simulations, unfortunately, has so far remained a computationally significant challenge, as it involves simulating long polymers and correspondingly long time-scales. Nevertheless, in a recent publication (16) we measured the dwell times in a *dynamical* self-avoiding polymer model wherein the polymers perform reptation and Rouse dynamics, and found that the mean dwell time scales as $N^{2.4 \pm 0.05}$, in clear contradiction to the mean-field results (14) as well as recent Langevin dynamics based simulation results (19).

Given the fact that the equilibration time-scale for a polymer constituted of N sequential monomers scales as $N^{1+2\nu}$, where $\nu = 0.588$ is the growth exponent for self-avoiding walks (20) (we verify this result with our polymer model in Sec. II.A), it seems that our scaling results in Ref. (16) serves to further confuse the issue of polymer equilibration during translocation, for the following reason. Our result of mean dwell time scaling as $N^{2.4 \pm 0.05}$ (16) implies that the equilibration time-scale is smaller than the dwell time-scale, which in turn indicates that perhaps one can indeed use mean-field theories in order to correctly describe the translocation process; and if one does so, one arrives at a different scaling behaviour for the mean dwell time (than $N^{2.4 \pm 0.05}$).

The purpose of this paper is to delve deep into the microscopics of the translocation dynamics to resolve the issues related to polymer equilibration and translocation. Our main finding is that the microscopic dynamics of the polymer during translocation is anomalous: in the sense that the microscopic motion of the reaction co-ordinate m *cannot* be described by a Fokker-Planck type equation (which only takes into account the diffusive and drift motions of the reaction-coordinate), as done in the mean-field theories. The reason behind this is that there are strong memory effects in the microscopic motion of the reaction co-ordinate. Our characterization of the anomalous dynamics of the reaction co-ordinate yields an important (and surprising!) conclusion; namely

that although the equilibration time-scale is smaller than the dwell time-scale, one cannot use mean-field theories (with particular reference to Fokker-Planck equation) to describe the translocation process.

Having said this, we note that the idea of anomalous dynamics of the polymer is not new. In Ref. (18), the authors already noted this, and based on their simulation results on mean dwell time, they conjectured (indirectly) the characteristics of the anomalous dynamics. Another recent work (21) envisaged certain forms of the anomalous dynamics and formulated a Fokker-Planck type equation to describe it. In this paper however, the anomalous dynamics of the polymer is characterized *directly*. In this matter, we do not find the mathematical formulation of Ref. (21) useful. Yet, we demonstrate that it is possible to recover the scaling of the mean dwell time with N from the anomalous dynamics of the reaction co-ordinate, and note that the results in this paper reconfirm our earlier scaling results in Ref. (16).

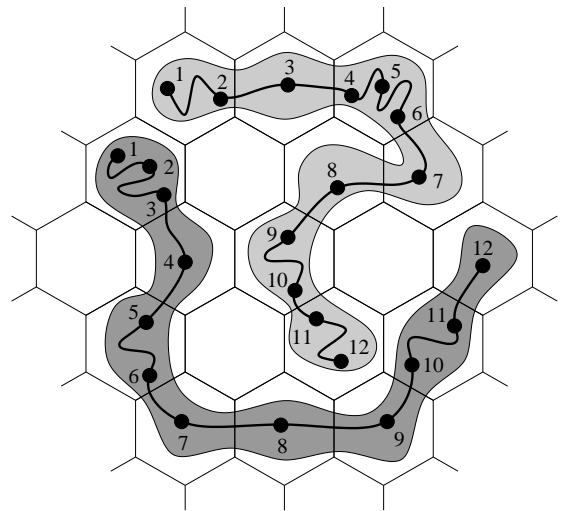


FIG. 2 Illustration of the two-dimensional version of the lattice polymer model. In the upper polymer, interior monomers 2, 4, 6, 9, 10 and 11 can either diffuse along the polymer backbone, or move sideways; monomer 7 can join either 6 or 8; the end monomers 1 and 12 can move to any vacant nearest-neighbor site. In the lower polymer, interior monomers 3, 5, 6, 10 and 11 can either diffuse along the tube, or move sideways; monomer 1 can move to any vacant nearest-neighbor site, and monomer 12 can join its neighbor 11. All other monomers are not mobile.

This paper is divided in four sections. In Sec. II we detail the dynamics of our polymer model, and outline its implications on physical processes including equilibration of phantom and self-avoiding polymers. In Sec. III we elaborate on a novel way of measuring the mean dwell time that allows us to take N up to 1000. In Sec. IV we describe and characterize the anomalous dynamics of translocation and check consistency of our results in Ref. (16). Finally in Sec. V we end this paper with a discussion.

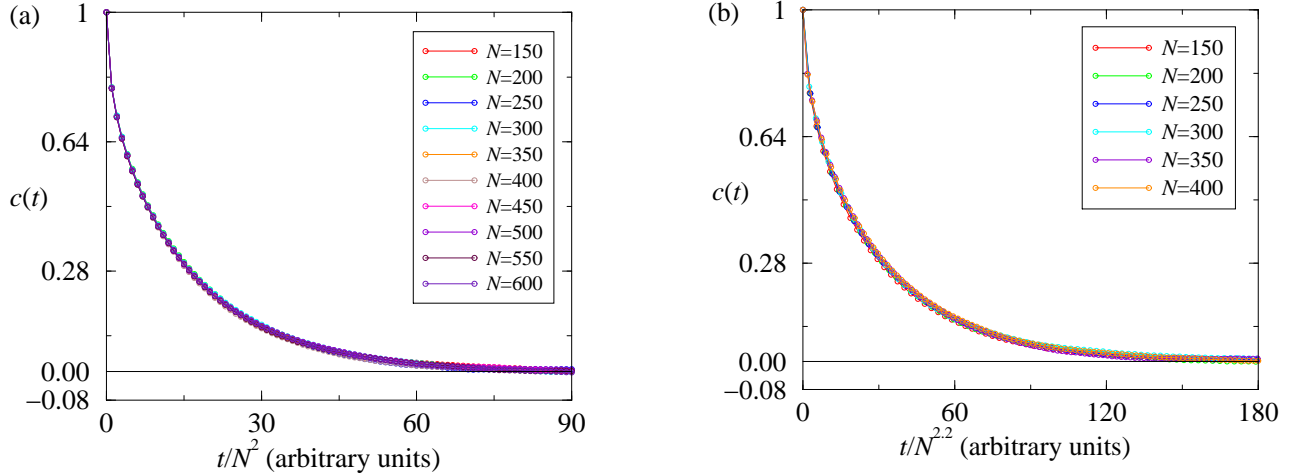


FIG. 3 Collapse of $c(t)$ for different values of N , showing that the equilibration times for phantom and self-avoiding polymers scale as N^2 and $N^{2.2}$ respectively. Here N is the polymer length. (a) Data for phantom polymers, simulations were run with the same definition of time for all values of N ; to achieve the data collapse, the times were then scaled by a factor N^2 . (b) Data for self-avoiding polymers, simulations were run with the same definition of time for all values of N ; to achieve the data collapse, the times were scaled by a factor $N^{2.2}$. Note that the units of time are arbitrary and clearly not important for the scaling of polymer equilibration times.

II. OUR POLYMER MODEL

Over the last years, we have developed a highly efficient simulation approach of polymer dynamics. This approach is made possible via a lattice polymer model, based on Rubinstein's repton model (24) for a single reptating polymer, with the addition of sideways moves (Rouse dynamics) and entanglement. A detailed description of this lattice polymer model, its computationally efficient implementation and a study of some of its properties and applications can be found in Refs. (22; 23).

In this model, polymers consist of a sequential chain of monomers, living on a FCC lattice. Monomers adjacent in the string are located either in the same, or in neighboring lattice sites. The polymers are self-avoiding: multiple occupation of lattice sites is not allowed, except for a set of adjacent monomers. The polymers move through a sequence of random single-monomer hops to neighboring lattice sites. These hops can be along the contour of the polymer, thus explicitly providing reptation dynamics. They can also change the contour "sideways", providing Rouse dynamics. Time in this polymer model is measured in terms of the number of attempted reptation moves. A two-dimensional version of our three-dimensional model is illustrated in fig. 2.

A. Influence of the accelerated reptation moves on polymer dynamics

From our experience with the model we already know that the dynamical properties are rather insensitive to the ratio of the rates for Rouse vs. reptation moves (i.e.,

moves that alter the polymer contour vs. moves that only redistribute the stored length along the backbone). Since the computational efficiency of the latter kind of moves is at least an order of magnitude higher, we exploit this relative insensitivity by attempting reptation moves r times more often than Rouse moves; typical values are $r = 5$ or 10 , which correspond to a comparable amount of computational effort invested in both kinds of moves. Certainly, the interplay between the two kinds of moves is rather intricate (25). Recent work by Drzewinski and van Leeuwen on a related lattice polymer model (26) provides evidence that the dynamics is governed by $Nr^{-1/2}$, supporting our experience that, provided the polymers are sizable, one can boost one mechanism over the other quite a bit (even up to $r \sim N^2$) before the polymer dynamics changes qualitatively.

In order to further check the trustworthiness of this model, we use it to study the equilibration properties of polymers with one end tethered to a fixed infinite wall (this problem relates rather directly to that of a translocating polymer: for a given monomer threaded into the pore, the two segments of the polymer on two sides of the membrane behave simply as two independent polymer chains; see Fig. 1). This particular problem, wherein polymer chains (of length N) undergo pure Rouse dynamics (i.e., no additional reptation moves) is a well-studied one: the equilibration time is known to scale as $N^{1+2\nu}$ for self-avoiding polymers and as N^2 for phantom polymers. To reproduce these results with our model we denote the vector distance of the free end of the polymer w.r.t. the tethered end at time t by $\mathbf{e}(t)$, and define the

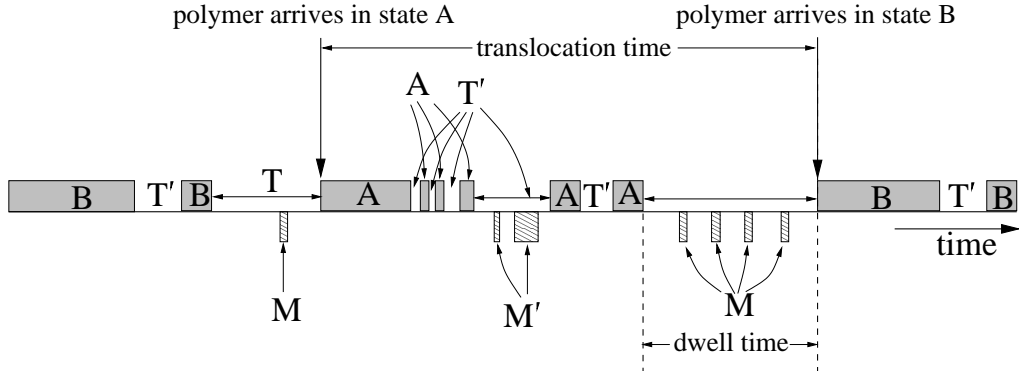


FIG. 4 A typical translocation process of the polymer as for our system the polymers move repeatedly back and forth between cells A and B. See Fig. 1 and text for the definitions of the states A, B, T, M, T' and M'.

correlation coefficient for the end-to-end vector as

$$c(t) = \frac{\langle \mathbf{e}(t) \cdot \mathbf{e}(0) \rangle - \langle \mathbf{e}(t) \rangle \cdot \langle \mathbf{e}(0) \rangle}{\sqrt{\langle \mathbf{e}^2(t) - \langle \mathbf{e}(t) \rangle^2 \rangle \langle \mathbf{e}^2(0) - \langle \mathbf{e}(0) \rangle^2 \rangle}}. \quad (1)$$

The angular brackets in Eq. (1) denote averaging in equilibrium. The $\bar{c}(t)$ quantities appearing in Fig. 3 have been obtained by the following procedure: we first obtain the time correlation coefficients $c(t)$ for 32 independent polymers, and $\bar{c}(t)$ is a further arithmetic mean of the corresponding 32 different time correlation coefficients. For different values of N we measure $\bar{c}(t)$ for both self-avoiding and phantom polymers. When we scale the units of time by factors of N^2 and $N^{2.2}$ respectively for phantom and self-avoiding polymers, the $\bar{c}(t)$ vs. t curves collapse on top of each other. This is shown in Fig. 3. Note here that $1 + 2\nu = 2.175$, which is sufficiently close to 2.2, and in simulations of self-avoiding polymers [Fig. 2(b)] we cannot differentiate between $1 + 2\nu$ and 2.2.

III. TRANSLOCATION, DWELL AND UNTHREADING TIMES

Our translocation simulations are carried out only for self-avoiding polymers. For long polymers, full translocation simulations, i.e., having started in one of the cells (Fig. 1), finding the pore and distorting their shapes to enter the pore to finally translocate to the other side of the membrane are usually very slow. An uncoiled state, which the polymer has to get into in order to pass through the pore is entropically unfavourable, and therefore, obtaining good translocation statistics for translocation events is a time-consuming process. To overcome this difficulty, in Ref. (16), we introduced three different time scales associated with translocation events: translocation time, dwell time and unthreading time.

A. Translocation and dwell times

In states A and B (Fig. 1), the entire polymer is located in cell A, resp. B. States M and M' are defined as the states in which the middle monomer is located exactly halfway between both cells. Finally, states T and T' are the complementary to the previous states: the polymer is threaded, but the middle monomer is not in the middle of the pore. The finer distinction between states M and T, resp. M' and T' is that in the first case, the polymer is on its way from state A to B or vice versa, while in the second case it originates in state A or B and returns to the same state. The translocation process in our simulations can then be characterized by the sequence of these states in time (Fig. 4). In this formulation, the mean dwell time $\langle \tau_d \rangle$ is the mean time that the polymer spends in states T, while the translocation time $\langle \tau_t \rangle$ is the mean time starting at the first instant the polymer reaches state A after leaving state B, until it reaches state B again. As found in Ref. (16), $\langle \tau_d \rangle$ and $\langle \tau_t \rangle$ are related to each other by the relation

$$\langle \tau_t \rangle = V \langle \tau_d \rangle N^{1+\gamma-2\gamma_1}, \quad (2)$$

where $\gamma = 1.1601$, $\gamma_1 = 0.68$ and V is the volume of cell A or B (see Fig. 1).

B. Unthreading time and its relation to dwell time

The mean unthreading time $\langle \tau_u \rangle$ is the average time that either state A or B is reached from state M (not excluding possible recurrences of state M). Notice that in the absence of a driving field the mean times to unthread to state A equals the the mean times to unthread to state B, due to symmetry. The advantage of introducing unthreading time is that when one measures the unthreading times, the polymer is at the state of lowest entropy at the start of the simulation and therefore simulations are fast and one can obtain good statistics on unthreading times fairly quickly. Additionally, the dwell

and unthreading times are related to each other, as outlined below, and using this relation one is able to reach large values of N for obtaining the scaling of the mean dwell time.

The main point to note that the mean dwell time can be decomposed into three parts as

$$\langle \tau_d \rangle = \langle \tau_{A \rightarrow M} \rangle + \langle \tau_{M \leftarrow M} \rangle + \langle \tau_{M \rightarrow B} \rangle, \quad (3)$$

whereas mean unthreading time can be decomposed into two parts as

$$\langle \tau_u \rangle = \langle \tau_{M \leftarrow M} \rangle + \langle \tau_{M \rightarrow B} \rangle. \quad (4)$$

Here $\langle \tau_{A \rightarrow M} \rangle$, $\langle \tau_{M \leftarrow M} \rangle$ and $\langle \tau_{M \rightarrow B} \rangle$ respectively are the mean first passage time to reach state M from state A, mean time between the first occurrence at state M and the last occurrence of state M with possible reoccurrences of state M, and the mean first passage time to reach state B from state M without any reoccurrence of state M. Notice that $\langle \tau_{A \rightarrow M} \rangle = \langle \tau_{M \rightarrow B} \rangle$ due to symmetry, and all quantities on the r.h.s. of Eqs. (3) and (4) are strictly positive. We therefore arrive at the inequality

$$\langle \tau_u \rangle < \langle \tau_d \rangle < 2\langle \tau_u \rangle. \quad (5)$$

Since Eq. (5) is independent of polymer lengths, the mean dwell time scales with N in the same way as the mean unthreading time (27).

We note here that the main finding of this paper is that the dynamics of the reaction co-ordinate *cannot* be described by a Fokker-Planck type description with one-dimensional diffusion and drift (discussed in detail in Sec. IV), which prevents us from constructing a simple theoretical model of a single particle with diffusion-and-drift on a one-dimensional lattice to determine an equality relation between $\langle \tau_d \rangle$ and $\langle \tau_u \rangle$. Since such an equality relation crucially hangs on the measurement of the ratio $\langle \tau_{A \rightarrow M} \rangle / \langle \tau_{M \leftarrow M} \rangle$, without having to do the full polymer simulations, we find it impossible to obtain an equality relation between $\langle \tau_d \rangle$ and $\langle \tau_u \rangle$. Nevertheless, in view of the fact that the purpose of this paper is to relate the scaling $\langle \tau_d \rangle$ with N to the polymer's microscopic (anomalous) dynamics, we have decided not to further investigate such an equality relation.

IV. CHARACTERIZATION OF THE ANOMALOUS DYNAMICS OF THE REACTION CO-ORDINATE AND ITS RELATION TO $\langle \tau_d \rangle$

The reaction coordinate [the monomer number $m(t)$, which is occupying the pore at time t] a convenient choice for the description of the microscopic movements of the translocating polymer, since the important time-scales for translocation can be obtained from the time evolution of the reaction coordinate $m(t)$ as shown below. To delve deeper into its temporal behavior, we determine $P_{N,r}(m_1, m_2, \Delta t)$, the probability distribution that at time t a polymer of length N is in a configuration

for which monomer m_1 is threaded into the pore, and the polymer evolves at time $t + \Delta t$ into a configuration in which monomer m_2 is threaded into the pore. The subscript r denotes our parametrization for the polymer movement, as it determines the frequency of attempted reptation moves and the sideways (or Rouse) moves of the polymer. See Sec. II.A for details.

First, we investigate the shape of these probability distributions for various values of m_1 , m_2 and Δt , for different sets of N and r values. We find that as long as the Δt values are such that neither m_1 nor m_2 are too close to the end of the polymer, $P_{N,r}(m_1, m_2, \Delta t)$ depends only on $(m_2 - m_1)$, but the centre of the distribution is slightly shifted w.r.t. the starting position m_1 by some distance that depends on m_1 , N and r . This is illustrated in Fig. 5, where (on top of each other) we plot $P_{N,r}(m_1, m_2, \Delta t)$ for $m_1 = N/4, N/2$ and $3N/4$ at $\Delta t = 100$ time units, for $N = 400$, and $r = 10$, as well as the Gaussian distribution. Notice in fig. 5 that the distribution $P_{N,r}(m_1, m_2, \Delta t)$ differs slightly from Gaussian (the parameter for the Gaussian is calculated by least-square optimization). We find that this difference decreases with increasing values of Δt (not shown in this paper).

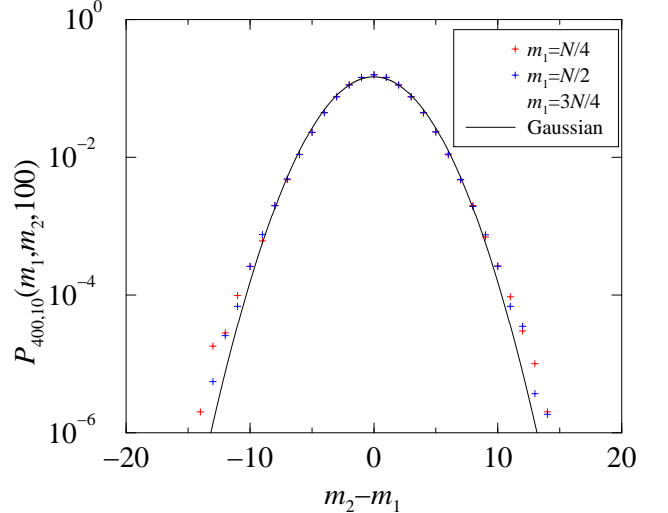


FIG. 5 $P_{N,r}(m_1, m_2, \Delta t)$ for $N = 400$ and $r = 10$, at $\Delta t = 100$. Note the data collapse when plotted as a function of $(m_2 - m_1)$. The distribution differs slightly from Gaussian.

We now define the mean $\langle m_2 - m_1 \rangle_{N,r}(m_1, \Delta t)$ and the standard deviation $\sigma_{N,r}(\Delta t)$ of the distribution $P_{N,r}(m_1, m_2, \Delta t)$ as

$$\begin{aligned} \langle m_2 - m_1 \rangle_{N,r}(m_1, \Delta t) &= \int dm_2 (m_2 - m_1) \times \\ &P_{N,r}(m_1, m_2, \Delta t); \\ \sigma_{N,r}^2(\Delta t) &= \int dm_2 (m_2 - m_1)^2 P_{N,r}(m_1, m_2, \Delta t) \\ &- [\langle m_2 - m_1 \rangle_{N,r}(m_1, \Delta t)]^2, \quad (6) \end{aligned}$$

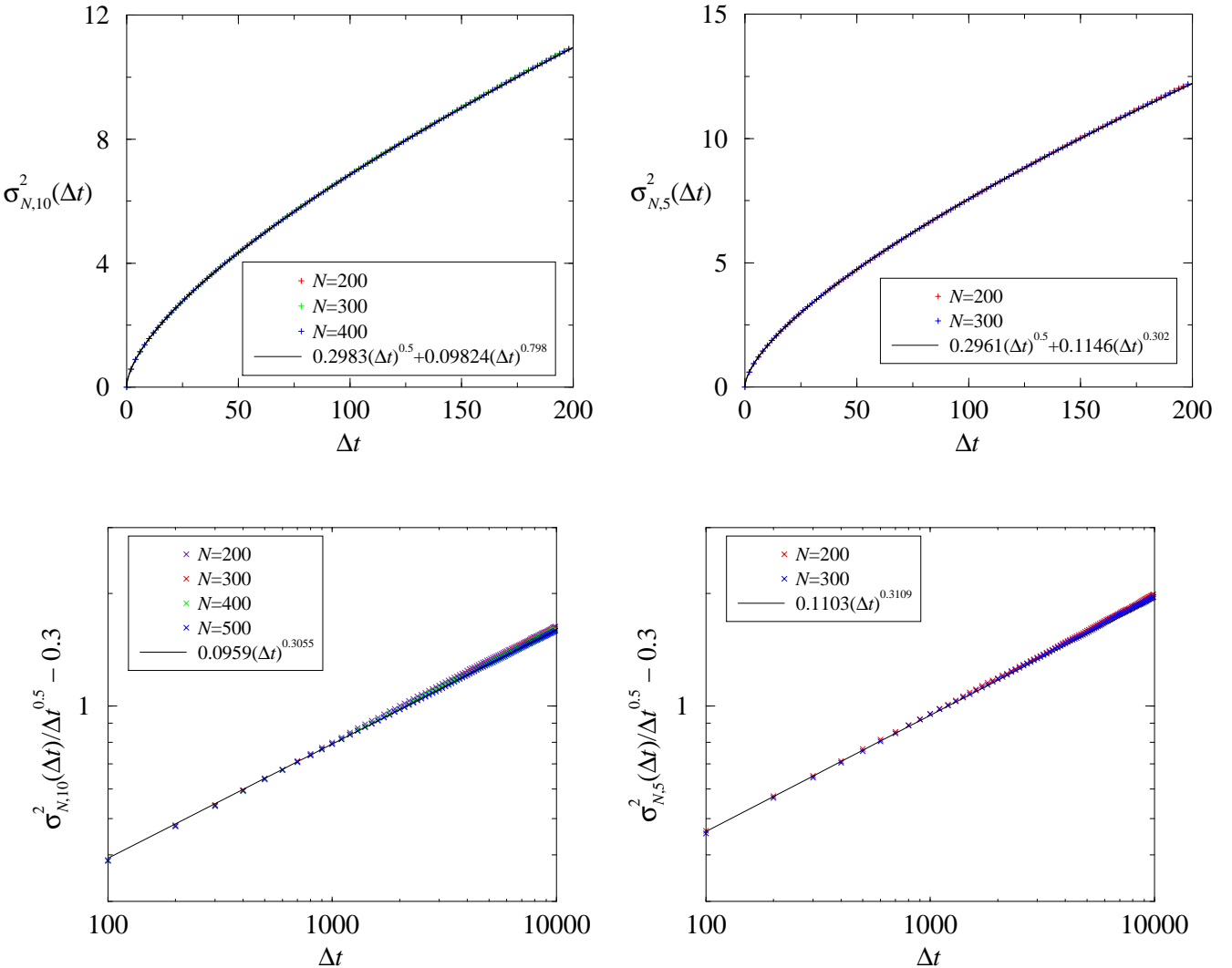


FIG. 6 Top panel: $\sigma_{N,r}^2(\Delta t)$ between $\Delta t = 0$ and $\Delta t = 200$ for different values of N , $r = 10$ (left) and $r = 5$ (right) [the data for part (i) of our statistical jackknifing procedure]. Notice the data collapse for different values of N . The fitted values of $k_r^{(s)}$, $k_r^{(l)}$ and α are also indicated. Bottom panel: Part (ii) of the data for $r = 10$ (left) and $r = 5$ (right); using the value $k_r^{(s)} = 0.3$, we again determine $k_r^{(l)}$ and α . The agreement of these values between the top and the bottom panel convinces us that $\alpha = 0.81 \pm 0.01$.

where the quantities within parenthesis on the l.h.s. of Eq. (6) denote the functional dependencies of the mean and the standard deviation of $(m_2 - m_1)$. We also note here that we have checked the skewness of $P_{N,r}(m_1, m_2, \Delta t)$, which we found to be zero within the scope of numerical calculations, indicating that $P_{N,r}(m_1, m_2, \Delta t)$ is symmetric in $(m_2 - m_1)$.

For a given value of r , in principle, both the mean and the standard deviation of $(m_2 - m_1)$ can be used to obtain the scaling of $\langle \tau_d \rangle$ with N , but the advantage of using $\sigma_{N,r}(\Delta t)$ for this purpose is that it is independent of m_1 . Since unthreading process at $m_1 = N/2$, the scaling of $\langle \tau_d \rangle$ with N is easily obtained by using the relation

$$\sigma_{N,r}(\langle \tau_u \rangle) \simeq N/2, \quad (7)$$

in combination with the fact that the scalings of $\langle \tau_d \rangle$ and $\langle \tau_u \rangle$ with N behave in the same way. Note here that Eq. (7) uses the fact that for an unthreading process the polymer only has to travel a length $N/2$ along its contour in order to leave the pore. In the limit $N \rightarrow \infty$, the scaling of $\langle \tau_d \rangle$ is then essentially given by the long-time behaviour of $\sigma_{N,r}(\Delta t)$, i.e., the behaviour of $\sigma_{N,r}(\Delta t)$ at large values of Δt .

The short time behaviour of $\sigma_{N,r}(\Delta t)$ is entirely determined by the reptation moves of the polymer. First of all, Rouse moves are not allowed for the monomers that are within the pore, and therefore time evolution of $m(t)$ (i.e., translocation) is only possible via reptation moves. In other words, we cannot set $r = 0$. Secondly, the reptation mechanism is essentially a transport mechanism for

“stored lengths” (24) along the polymer’s contour, and the stored lengths cannot pass each other. As a result, the dynamics of $m(t)$, governed by the movement of the stored lengths across the pore, is equivalent to a process known as “single-file diffusion” or “tagged particle diffusion”. Such dynamics should therefore be characterized by the anomalous diffusive scaling

$$\sigma_{N,r}(\Delta t) = k_{N,r}^{(s)}(\Delta t)^{1/4}, \quad (8)$$

where the superscript ‘(s)’ stands for short time behaviour.

The long time behaviour of $\sigma_{N,r}(\Delta t)$ is more complicated, as it involves contribution from both Rouse (away from the pore) and reptation moves of the polymer. We do not have an theoretical description of it, so we determine the long time behaviour of $\sigma_{N,r}(\Delta t)$ by the following empirical procedure. First we use the $\sigma_{N,r}(\Delta t)$ data for short times; the $\sigma_{N,r}(\Delta t)$ data for different N collapse on top of each other, indicating that $k_{N,r}^{(s)} \equiv k_r^{(s)}$. This collapse can be seen for two different values of r , namely 5 and 10 in Fig. 6 (top panel). Based on the theoretical description of short time behaviour in Eq. (8) and the data collapse at short times in Fig. 6 (top panel), we then conjecture

$$\sigma_{N,r}^2(\Delta t) = [k_r^{(s)}]^2 (\Delta t)^{1/2} + k_r^{(l)}(\Delta t)^\alpha, \quad (9)$$

where the superscript ‘(l)’ in Eq. (9) stands for long time behaviour.

Next, to test this conjecture we employ the so-called “statistical jackknifing”. In the present case, the idea behind this is to divide the $\sigma_{N,r}^2(\Delta t)$ data from $\Delta t = 0$ to $\Delta t = 10000$ into two parts and test our conjecture in (9) *independently* on these two parts. Part (i) consists of $\sigma_{N,r}^2(\Delta t)$ data from $\Delta t = 0$ to $\Delta t = 200$ in intervals of $\Delta t = 2$ and part (ii) consists of $\sigma_{N,r}^2(\Delta t)$ data from $\Delta t = 100$ to $\Delta t = 10000$ in intervals of $\Delta t = 100$.

For the data in part (i), in view of the collapse for different values of N [Fig. 6 (top panel)], for $N = 400$, $r = 10$, and $N = 300$, $r = 5$, we determine $k_r^{(s)}$, $k_r^{(l)}$ and α , using least-square optimization. This leads us to the following values: $[k_r^{(s)}]^2 = 0.3$ independent of r , $[k_5^{(l)}]^2 = 0.11$, $[k_{10}^{(l)}]^2 = 0.1$ and $\alpha = 0.8$. Note here that the independence of $k_r^{(s)}$ on r is a confirmation of the fact that the short time behaviour of $\sigma_{N,r}(\Delta t)$ is *entirely* determined by the reptation moves of the polymer: since time in this polymer model is measured in terms of the number of attempted reptation moves, how frequently Rouse moves are attempted (away from the pore) w.r.t. the reptation ones should not affect the value of $k_r^{(s)}$.

Finally, we consider the data in part (ii), and using the value of $k_r^{(s)} = 0.3$, we plot $\sigma_{N,r}^2(\Delta t)/(\Delta t)^{1/2} - [k_r^{(s)}]^2$ as a function of Δt . The data for different values of N collapse again [Fig. 6 (bottom panel)], and for $N =$

500, $r = 10$, and $N = 400$, $r = 5$, we determine $k_r^{(l)}$ and α , using the optimization program within gnuplot. The consistency of the resulting values, $[k_5^{(l)}]^2 = 0.11$, $[k_{10}^{(l)}]^2 = 0.096$ and $\alpha \simeq 0.8$, with the ones obtained from convince us that the value of α , which we need to obtain $\langle \tau_d \rangle$ in the limit $N \rightarrow \infty$ using Eq. (9), is given by (including error bars)

$$\alpha = 0.81 \pm 0.01. \quad (10)$$

Our results above have many significant implications:

- (i) The complete polymer configuration retains some memory of previous values of the reaction coordinate, dating back over the whole translocation process. In the one-dimensional reaction coordinate space, this translates into a memory kernel and sub-diffusive behaviour.
- (ii) Since $\alpha < 1$, the diffusion in reaction-coordinate space is anomalous. This means that the dynamics of the polymer in terms of its reaction co-ordinate *cannot* be captured by a Fokker-Planck equation, i.e., mean-field approaches (13; 14; 15) that are based on Fokker-Planck equation do not capture the translocation process and consequently they do *not* describe the scaling of the mean dwell time with polymer length correctly.
- (iii) We also emphasize here that while we have not been able to find a description in terms of a more complicated Fokker-Planck type equation for the anomalous dynamics, an earlier work (21) that envisaged certain forms of the anomalous dynamics are not useful to describe the anomalous dynamics we found in this model.
- (iv) The fact that α is independent of r demonstrates the robustness of our polymer model to study translocating polymers. We repeat here that empirically we found $r = 10$ yields the fastest runtime of our code; this was the same value used in our earlier work (16). Using $r = 5$ makes the code approximately three times slower in the best case.
- (v) Equations (7) and (9) together imply that $\langle \tau_d \rangle$ scales as $N^{2/4\alpha}$, i.e., as $N^{2.46 \pm 0.03}$. Within statistical error bars this is in agreement with our earlier result (16).
- (vi) As shown by the data collapse in Fig. 6 for various N , $\sigma_{N,r}(\Delta t)$ becomes independent of N very quickly above $N \sim 100$. Nevertheless, in Ref. (16) we had to take N to above 1000 in order to obtain the true scaling of $\langle \tau_d \rangle$ with N . This is simply due to the fact that the difference between the two exponents α and $1/2$ in Eq. (9) is not a large. To obtain the true scaling of $\langle \tau_d \rangle$ with N we therefore need to get rid of the finite N corrections to $\langle \tau_d \rangle \sim N^{2/\alpha}$, which requires using very large values of N .

V. CONCLUSION

In summary, our main finding in this paper is that the microscopic dynamics of the polymer during translocation is anomalous: in the sense that the microscopic motion of the reaction co-ordinate m *cannot* be described by a Fokker-Planck type equation (which only takes into account the diffusive and drift motions of the reaction-coordinate). The reason behind this is that there are strong memory effects in the microscopic motion of the reaction co-ordinate. The idea that translocation dynamics may be anomalous is not new; nevertheless, here we develop a direct characterization method for it for the first time. Our characterization of the anomalous dynamics of the polymer reconfirms our earlier scaling results in Ref. (16).

In essence, the results in this paper robustly demonstrates that

- (a) Although equilibration time scale of a polymer is smaller than its dwell time scale, quasi-equilibrium condition cannot be assumed as the starting point, as has been done in the mean-field theories.
- (b) A Fokker-Planck equation or a Fokker-Planck type equation existing in translocation literature cannot be used to describe the dynamics of the reaction co-ordinate, although both have been widely used as the starting point for quantitative theoretical analysis of translocation (mean-field theories arrive at a Fokker-Planck description of the reaction co-ordinate dynamics upon first converting translocation dynamics to a first-passage or Kramer's problem, and then assuming the quasi-equilibrium condition of the polymer during translocation).

References

- [1] B. Dreiseikermann, *Microbiol. Rev.* **58**, 293 (1994).
- [2] J. P. Henry *et al.*, *J. Membr. Biol.* **112**, 139 (1989).
- [3] J. Akimaru *et al.*, *PNAS USA* **88**, 6545 (1991).
- [4] D. Goerlich and T. A. Rappaport, *Cell* **75**, 615 (1993).
- [5] G. Schatz and B. Dobberstein, *Science* **271**, 1519 (1996).
- [6] J. J. Nakane, M. Akeson, A. Marziali, *J. Phys.: Cond. Mat.* **15**, R1365 (2003).

- [7] I. Szabò *et al.*, *J. Biol. Chem.* **272**, 25275 (1997).
- [8] B. Hanss *et al.*, *PNAS USA* **95**, 1921 (1998).
- [9] Yun-Long Tseng *et al.*, *Molecular Pharm.* **62**, 864 (2002).
- [10] J. M. Tsutsui *et al.*, *Cardiovasc. Ultrasound* **2**, 23 (2004).
- [11] W. T. Wickner and H. F. Lodisch, *Science* **230**, 400 (1995).
- [12] S. M. Simon and G. Blobel, *Cell* **65**, 1 (1991); D. Goerlich and I. W. Mattaj, *Science* **271**, 1513 (1996); K. Verner and G. Schatz, *Science* **241**, 1307 (1988).
- [13] P. J. Sung and W. Park, *Phys. Rev. E* **57**, 730 (1998); M. Muthukumar, *Phys. Rev. Lett.* **86**, 3188 (2001).
- [14] P. J. Sung and W. Park, *Phys. Rev. Lett.* **77**, 783 (1996); M. Muthukumar, *J. Chem. Phys.* **111**, 10371 (1999).
- [15] D. K. Lubensky and D. R. Nelson, *Biophys. J.* **77**, 1824 (1999); P. J. Park and W. Sung, *J. Chem. Phys.* **108**, 3013 (1998); E. Slonkina and A. B. Kolomeisky, *J. Chem. Phys.* **118**, 7112 (2003).
- [16] J. K. Wolterink, G. T. Barkema and D. Panja, *Phys. Rev. Lett.* **96**, 208301 (2006).
- [17] J. Kasianowicz *et al.*, *PNAS USA* **93**, 13770 (1996); E. Henrickson *et al.*, *Phys. Rev. Lett.* **85**, 3057 (2000); A. Meller *et al.*, *Phys. Rev. Lett.* **86**, 3435 (2001); M. Akeson *et al.*, *Biophys. J.* **77**, 3227 (1999); A. Meller *et al.*, *PNAS USA* **97**, 1079 (2000); A. J. Storm *et al.*, *Nanoletters* **5**, 1193 (2005).
- [18] J. Chuang *et al.*, *Phys. Rev. E* **65**, 011802 (2002); Y. Kantor and M. Kardar, *Phys. Rev. E* **69**, 021806 (2004).
- [19] I. Huopaniemi, K. Luo, T. Ala-Nissila, S.-C. Ying, *J. Chem. Phys.* **125** 124901 (2006).
- [20] The exponent ν is also known as the Flory exponent and sometimes also referred to as the "swelling exponent".
- [21] R. Metzler and J. Klafter, *Biophys. J.* **85** 2776 (2003).
- [22] A. van Heukelum and G. T. Barkema, *J. Chem. Phys.* **119**, 8197 (2003).
- [23] A. van Heukelum *et al.*, *Macromol.* **36**, 6662 (2003); J. Klein Wolterink *et al.*, *Macromol.* **38**, 2009 (2005).
- [24] M. Rubinstein, *Phys. Rev. Lett.* **59**, 1946 (1987); T. A. J. Duke, *Phys. Rev. Lett.* **62**, 2877 (1989).
- [25] J. Klein Wolterink and G. T. Barkema, *Mol. Phys.* **103**, 3083 (2005).
- [26] A. Drzewinski and J.M.J. van Leeuwen, e-print archive cond-mat/0609281 (2006).
- [27] In Ref. (16) we overlooked the $\langle \tau_{M \leftrightarrow M} \rangle$ term of Eq. (3) to (mistakenly) deduce $\langle \tau_d \rangle = 2\langle \tau_u \rangle$. Nevertheless, due to the independence of Eq. (5) on N our results for the scaling of $\langle \tau_d \rangle$ in Ref. (16) remain unaffected.